

# Design of aperture-coupled microstrip patch antenna array fed by SIW for 60 GHz band

ISSN 1751-8725


Received on 28th April 2015

Revised on 22nd September 2015


Accepted on 27th September 2015

doi: 10.1049/iet-map.2015.0296

www.ietdl.org

Tomas Mikulasek , Jaroslav Lacik, Jan Puskely, Zbynek Raida

Department of Radio Electronics, Brno University of Technology, Technicka 12, 616 00 Brno, Czech Republic

 E-mail: mikulasekt@feec.vutbr.cz

**Abstract:** This study deals with a design procedure and achieved parameters of a microstrip patch antenna array fed by a substrate integrated waveguide (SIW) operating at V-band. The antenna array consists of  $6 \times 8$  microstrip patch antennas which are aperture coupled with an SIW-based feeding network. The antenna design is performed in a full-wave electromagnetic solver (ANSYS HFSS) for the operation frequency 60 GHz. The design procedure of the proposed antenna array comprises the analysis of an isolated radiating element, the synthesis of a linear array, and the development of an SIW-based power divider. At the operation frequency 60 GHz, a fabricated prototype has an impedance bandwidth of 1.8% for a reflection coefficient lower than  $-10$  dB, a gain of 21.6 dBi, and a low sidelobe level below  $-23$  dB in the E-plane and H-plane.

## 1 Introduction

The main features of the 60 GHz ISM frequency band (60 GHz band) are obvious: license free use, relatively wide allocated contiguous bandwidth, and very high radio wave absorption caused by the resonance of oxygen molecules. Despite the high attenuation that allows excellent frequency reuse, the challenges associated with this channel motivate commercial deployment of short-range wireless local area networks, wireless personal area networks, wireless body area networks, vehicular networks, or point to point links with high transmission capacity [1].

High-gain antennas with high radiation efficiency are usually required for such applications. In many cases, the antennas are based on substrate integrated waveguide (SIW) technology as slot antennas, microstrip patch antennas (MPAs), dielectric resonator antennas (DRAs), etc. SIW is exploited due to its low loss, low cost, ease of integration with planar circuits, and advantages similar to conventional metallic rectangular waveguides (RWGs), for example, high quality factor and high power capacity [2–7]. Thanks to its self-consistent electrical shielding, SIW is very popular for designing many types of antennas and circuits [8].

Longitudinal slot antenna arrays fed by an SIW-based power divider features a single layer structure, high gain and narrow operation bandwidth [9–11]. They are usually designed using Elliott's design procedure [12] that allows feeding slots with a defined weighted power and thus ensures low side lobe level (SLL). In [9], the antenna array consisting of  $16 \times 16$  slots achieved very low SLL below  $-30$  dB and a high gain over 24 dBi at 10 GHz. In [10], a 60 GHz antenna array consisting of  $12 \times 12$  slots achieved a  $-25$  dB SLL in the H-plane,  $-15$  dB SLL in the E-plane, a gain of about 22 dBi, and a 4.2% bandwidth for the  $-10$  dB reflection coefficient.

A longitudinal slot placed in the broad wall of an SIW can be utilised for exciting antenna structures as DRAs [13, 14] or MPAs [15–18]. Thanks to SIW feeding, the parasitic radiation of the feeding part is minimised and thus the radiation pattern of the DRA or MPA is minimally affected. Any additional shielding of the feeding part is not required in comparison with, for example, the microstrip line feeding technique. In addition, the antenna structure fed by SIW is much thinner and the SIW-based feeding opens the possibility of implementing DRAs and MPAs into arrays in the millimetre-wave band [14, 15, 18–23].

DRA arrays fed by SIW have been intensively studied [14], however, their rugged profile can limit their usage in many

application cases where low profile antennas are required. In addition, its cost and demands on fabrication tolerances naturally grows with frequency. Compared with DRAs fed by SIW, MPAs fed by SIW have higher application potential thanks to their low profile, thinner layout, or higher degree of modification. For example, cavity-backed MPAs fed by SIW feature a high gain in a wide operation bandwidth; however, for narrow-band applications their design and fabrication procedure would be rather complicated due to its multilayer-nature structure [22, 23].

Formation of MPAs fed by SIW into an out-of-line series-fed (linear) array is advantageous from several points of view. The feeding network occupies a similar area as MPAs while MPAs can be excited using defined amplitude weighting. On the other hand, a higher number of elements in the linear array leads to decreasing operation bandwidth. In [15], the first antenna concept of a linear array consisting of eight aperture-coupled MPAs (AC-MPAs) fed by SIW was introduced. The antenna array achieved a 1.5% impedance bandwidth and a 15.8 dBi gain at 60 GHz. The radiation pattern indicated an SLL of about  $-13$  dB because of the uniform amplitude distribution. Although this antenna array is rather complicated for design, the paper includes no related information about the design procedure and no experimental verification.

In this paper, we present a design procedure of a planar array of aperture-coupled microstrip patch antennas (AC-MPAs) fed by SIW operating at 60 GHz band. Compared with [15], the linear AC-MPAA fed by SIW is extended to a planar array, complemented by a power divider, and verified by the measurements of a real prototype. This paper is organised as follows. The antenna structure is described in Section 2. The design procedure for the antenna array comprising implementation of amplitude distribution and its simulation results are presented in Section 3. Simulated results of the proposed antenna array are experimentally verified using measurement in Section 4. Finally, Section 5 concludes this paper.

## 2 Antenna configuration

The structure of the AC-MPAA fed by SIW is shown in Fig. 1. The antenna consists of the planar array containing a  $6 \times 8$  AC-MPA placed on the top substrate and fed by an SIW-based feeding network integrated in the bottom substrate. The antenna is fed by a waveguide on the left-hand side. A six-way power divider ensures in-phase and non-uniform feeding for the linear arrays to suppress

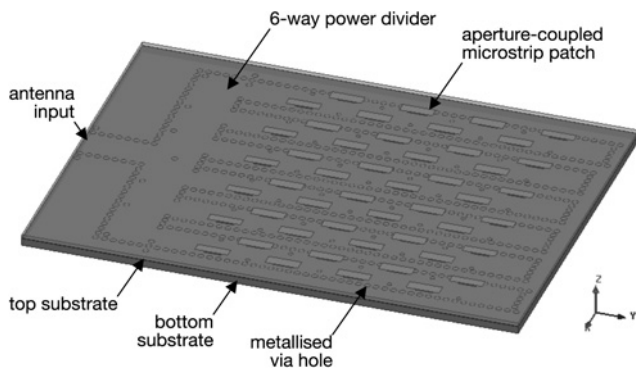


Fig. 1 Structure of  $6 \times 8$  AC-MPAA fed by SIW

side-lobes in the particular radiating plane (E-plane). In the perpendicular radiating plane (H-plane), an amplitude distribution for exciting the array elements is also implemented. The design of each antenna part is described in the next section.

### 3 Design procedure and simulation results

This section describes the design procedure and the simulation results of the antenna array and the SIW-based power divider. The presented simulation results were achieved using the full-wave electromagnetic simulator ANSYS HFSS. The design of the antenna is performed for the operation frequency of 60 GHz and SLL of  $-25$  dB.

#### 3.1 Parameter extraction of isolated radiator

The single antenna element of the AC-MPAA fed by SIW is depicted in Fig. 2. It consists of two dielectric layers, an SIW layer and a patch layer. The rectangular microstrip patch is placed on the top surface of the patch layer and it is aperture coupled with the dielectric-filled RWG integrated in the SIW layer. This antenna configuration has been described and investigated in detail in [17]. The AC-MPA fed by SIW is complemented by a metallised via hole with diameter  $d_v$  and offset  $x_v$  from the centre line of the RWG. The metallised via hole is integrated in the RWG for purposes of impedance matching of each antenna element.

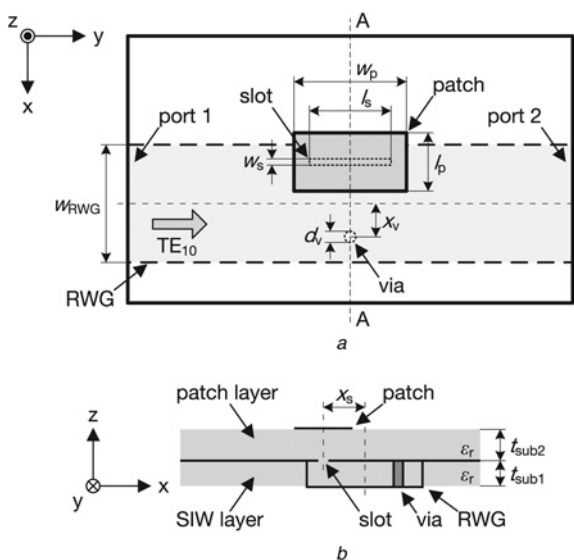


Fig. 2 Isolated AC-MPA fed by dielectric-filled RWG

a Top view  
b Section A-A (i.e. the cut plane of the structure according to Fig. 2a)

Considering the Elliott's design procedure for the slot waveguide array [12], a similar design approach is exploited for the design of an AC-MPAA fed by SIW because the AC-MPA fed by SIW can also be represented by a shunt element with an active admittance  $Y$ . The self-admittance of an isolated antenna element is extracted using the structure shown in Fig. 2. Regarding the equivalence of an SIW with a dielectric-filled RWG [4], the MPA is aperture-coupled with an equivalent dielectric-filled RWG to reduce computational time of the simulation runtime. The self-admittance  $Y$  of the isolated radiator normalised to the characteristic conductance  $G_0$  of the RWG is obtained by properly selecting the slot length  $l_s$  and the patch length  $l_p$  and then it is given by [12]

$$\frac{Y}{G_0} = \frac{G}{G_0} + j \frac{B}{G_0} = \frac{-2s_{11}}{1 + s_{11}}. \quad (1)$$

#### 3.2 Procedure of antenna array design

The antenna array is designed from low permittivity dielectric material Rogers RT/duroid 5880 ( $\epsilon_r = 2.2$  at 10 GHz) to achieve a maximal operation bandwidth. The thickness  $t_{\text{sub1}}$  of the SIW layer is 0.51 mm and the thickness  $t_{\text{sub2}}$  of the patch layer is 0.25 mm.

Initially, a linear array of eight self-resonant radiators shown in Fig. 3 is designed. At the operating frequency, the coupling slots are centred on the maximum peaks of the guided wave (half guided wave apart). The centre of the last slot is placed a quarter guided wave from the RWG end wall. The RWG operates with the fundamental mode  $TE_{10}$  with a cutoff frequency of approximately 43 GHz. The RWG width  $w_{\text{RWG}}$  is 2.35 mm.

This linear array of AC-MPAs fed by SIW is impedance matched through the desired frequency band while the sum of normalised conductances  $G/G_0$  of the AC-MPAs fed by SIW is equal to one at each operating frequency. Similarly, the sum of normalised susceptances  $B/G_0$  should be zero. To reach the required SLL of  $-25$  dB in the H-plane, an amplitude distribution is implemented for exciting the antenna elements. On the basis of the Dolph-Chebyshev distribution, the required values of  $G/G_0$  of the radiators are 0.23, 0.16, 0.08, and 0.03.

According to the procedure described in the previous section, the initial set of four AC-MPAs fed by SIW having the required values of  $G/G_0$  is achieved. Due to ignoring the mutual coupling between the antenna elements, it is sufficient to extract the normalised admittance  $Y/G_0$  only at the operating frequency. The antenna element in its initial configuration (without the via) [17] does not allow achieving zero normalized susceptance  $B/G_0$  due to its high capacitive character. Therefore, we use the metallised via hole inside the SIW as an additional tuning element that compensates for the capacitive character of the radiator and thus ensures to achieve a pure real normalised admittance  $Y/G_0$ . The initial set of AC-MPAs fed by SIW differ in the slot length  $l_s$  and the patch length  $l_p$ . The other parameters such as  $x_s$ ,  $w_s$ ,  $w_p$ ,  $x_v$ , and  $d_v$ , are shared by all.

The mutual coupling between the elements of the linear array causes a certain phase delay on the elements leading to out of phase feeding. As a result, it degrades the impedance matching and radiation pattern (lower gain and higher side lobes). The in-phase feeding is provided by changing the position of the via  $x_v$  while the electric field distribution on the microstrip patch is in-phase with other microstrip patches. This phase correction is proved using the

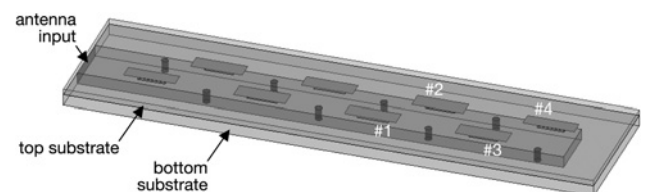
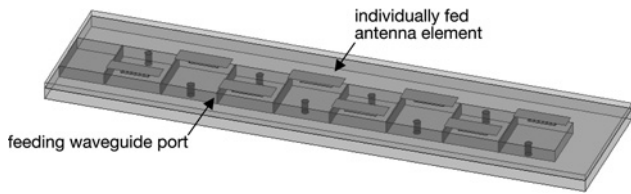
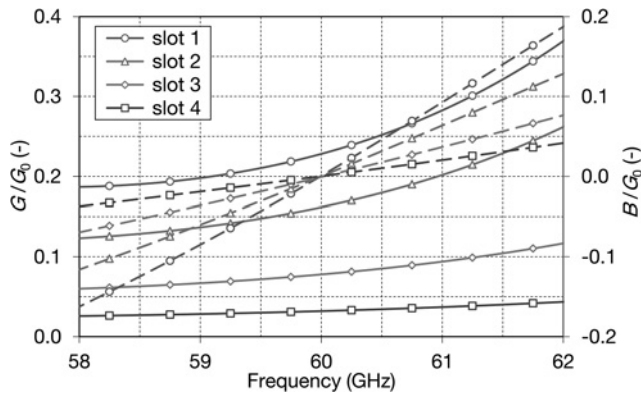


Fig. 3 Structure of linear AC-MPAA fed by SIW



**Fig. 4** Structure of individually excited AC-MPAs fed by SIW



**Fig. 5** Simulated normalised self-admittance of isolated radiating element (solid line– $G/G_0$ , dash line– $B/G_0$ )

structure shown in Fig. 4 where each array element is individually excited by waveguide port. The separation of the antenna elements is kept (a half guided wave apart) to ensure the same exterior (electromagnetic) mutual coupling in the H-plane between adjacent antenna array elements. The feeding SIWs are about half guided wave long and the centre of the slot is at a distance of a quarter guided wave from the end of the appropriate SIW. Then, using the procedure described in the previous section, a new set of four AC-MPAs fed by SIW satisfying the required values of  $G/G_0$  is achieved for new values of  $x_v$  by changing  $l_s$  and  $l_p$ .

A linear array with new values of  $l_p$ ,  $l_s$ , and  $x_v$ , is simulated. Satisfactory results of this modified antenna array are usually achieved after one iterating step. In Fig. 5, the resultant normalised components of  $Y/G_0$  of isolated antenna elements agree with the required ones. The simulated results of the linear AC-MPAA fed by SIW with the parameters summarised in Table 1 are depicted in Fig. 6. The simulated reflection coefficient indicates an impedance bandwidth of 2.3% for  $s_{11} < -10$  dB. It is expected from Fig. 5 that the metallised via holes to compensate for the capacitive effect of the slots limit the bandwidth of the design due to a high dependence of  $Y/G_0$  on frequency. The radiation pattern shows the broadside gain of 14.5 dBi and H-plane SLL of  $-24.1$  dB.

In the planar antenna array structure (Fig. 1), the separation of the linear arrays is  $0.75\lambda_0$  at the operating frequency. Thanks to weak mutual coupling in the E-plane, any additional changes of the element parameters are not needed.

### 3.3 SIW-based power divider

Several approaches to design an SIW-based power divider have been published [9–11, 18, 24–26]. The structure of a six-way SIW power

**Table 1** Design parameters of array elements; dimensions in millimetres

$m$	$d_{vm}$	$l_{pm}$	$l_{sm}$	$w_{pm}$	$w_{sm}$	$x_{sm}$	$x_{vm}$
1	0.30	0.71	1.37	2.25	0.12	0.80	0.65
2	0.30	0.77	1.31	2.25	0.12	0.80	0.75
3	0.30	0.74	1.25	2.25	0.12	0.80	0.86
4	0.30	0.63	1.19	2.25	0.12	0.80	0.95

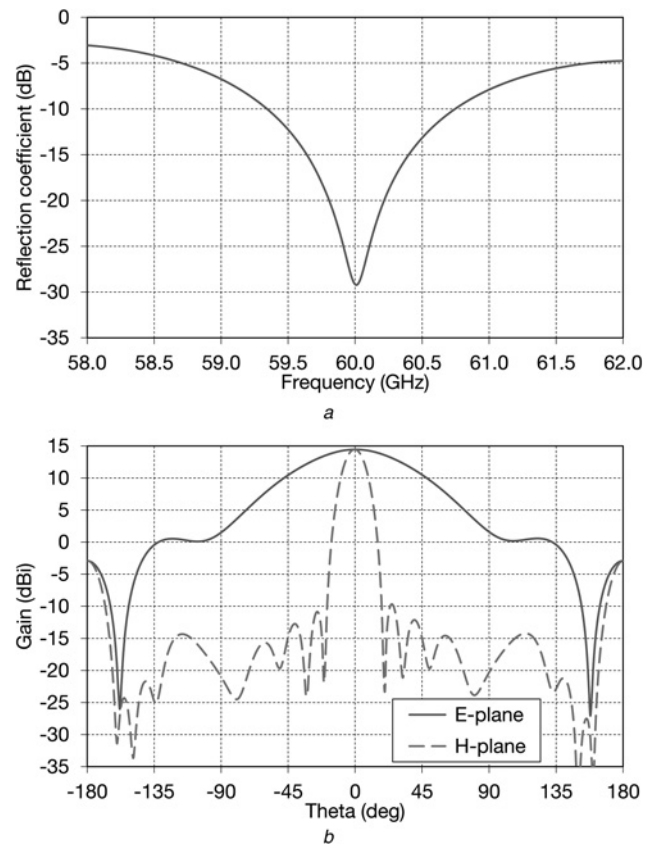


**Fig. 6** Simulated parameters of linear AC-MPAA fed by SIW

a Reflection coefficient at antenna array input  
b Radiation pattern at 60 GHz

divider is depicted in Fig. 7. Its configuration is similar to the one in [26]. The power divider consists of five T-junctions and two 90-degree bends that occupy a minimum space on the dielectric board. The operation bandwidth of the power divider reliably covers the operation bandwidth of the linear antenna array. To ensure the  $-25$  dB SLL, the required symmetrical amplitude distribution at the output branches of the power divider is 0.39–0.73–1.00 which corresponds to the Dolph-Chebyshev distribution for the same value of SLL. The output signals of the power divider are in-phase. Table 2 summarises the resultant design parameters of the power divider. Other parameters are  $d_{via} = 0.40$  mm,  $p_1 = 1.76$  mm,  $p_{via} = 0.60$  mm,  $s_x = 3.75$  mm,  $w_f = 3.61$  mm, and  $w_{SIW} = 2.65$  mm.

Fig. 8 depicts the simulated transmission characteristic of the designed power divider (Fig. 7). The magnitudes of the output signals at ports 2 to 4 correspond to the required power ratio and have negligible deviance from the required values at the centre frequency. At port 4, there is a 29-degree phase error in comparison with the others ports that could be compensated for by prolonging the output waveguide by 0.33 mm. The reflection

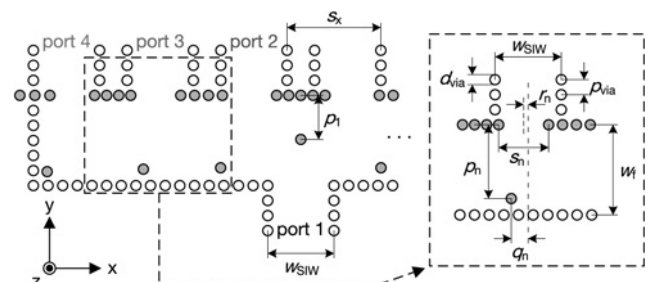


**Fig. 7** Six-way power divider configuration

**Table 2** Design parameters of six-way power divider; dimensions in millimetres

$n$	$p_n$	$q_n$	$r_n$	$s_n$
2	2.89	1.33	0.18	2.17
3	2.95	0.68	0.18	2.00
4	3.05	0.78	0.23	1.79

coefficient at the input of the power divider is lower than  $-20$  dB within the band from 58.5 to 61.5 GHz.

#### 4 Experimental results

The simulation results from ANSYS HFSS are validated by experimental measurement in this section. To verify the antenna operation experimentally, the antenna is fed by the standard RWG WR15 with a stepped RWG-to-SIW transition used in [27]. The transition is designed for minimum insertion loss in the operating band of the antenna array. The overall view of the fabricated

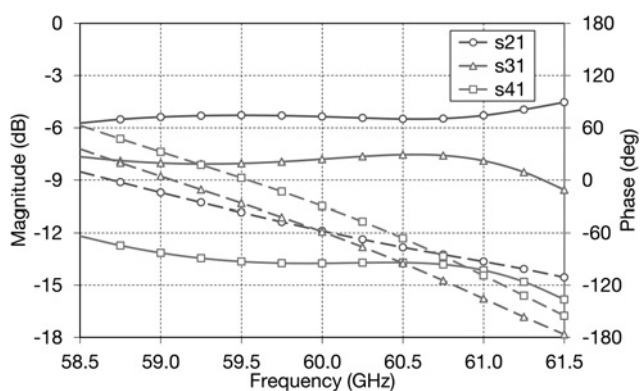
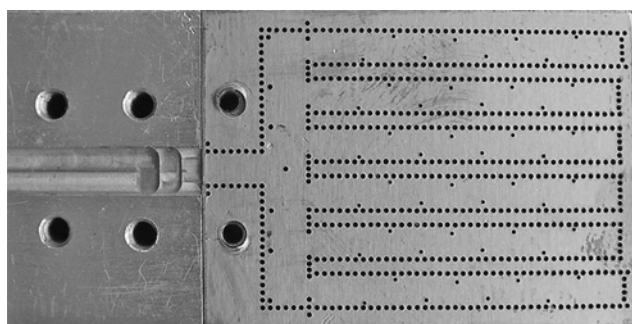
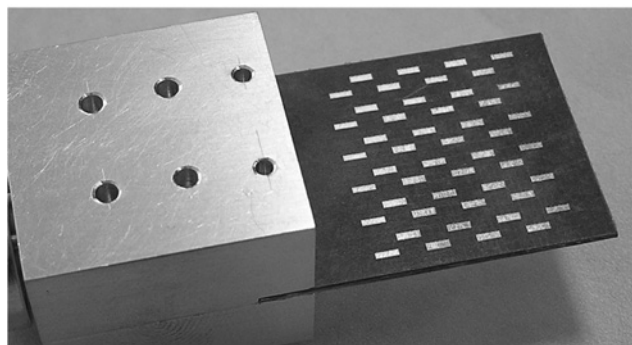


**Fig. 8** Transmission characteristic of six-way power divider; magnitude (solid line) and phase (dash line)



a



b

**Fig. 9** Fabricated prototype of AC-MPAA fed by SIW

a Bottom view (transition disassembled)  
b Perspective view

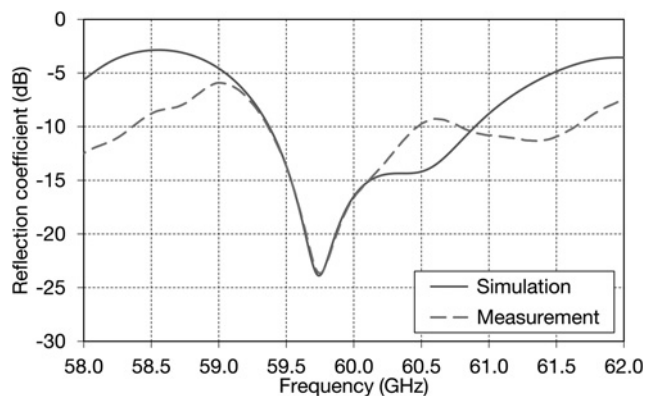
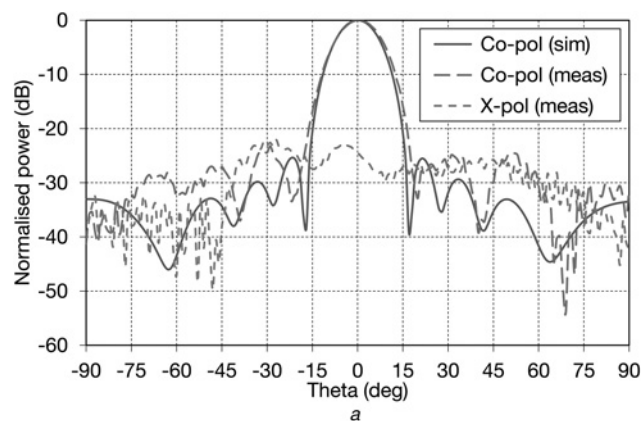


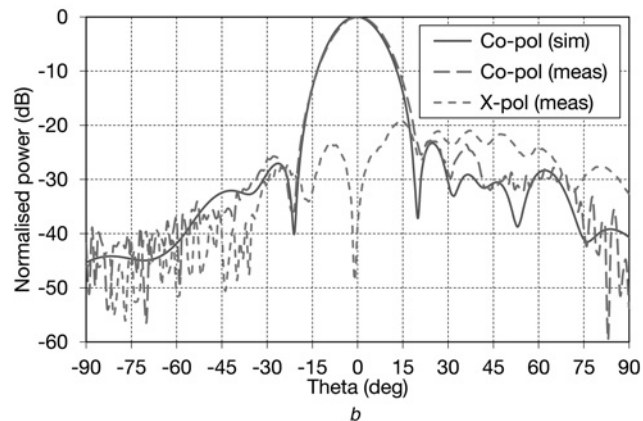
**Fig. 10** Reflection coefficient of fabricated AC-MPAA fed by SIW

antenna array is shown in Fig. 9. The antenna size (without the transition) is  $34.00 \text{ mm} \times 24.75 \text{ mm} \times 0.85 \text{ mm}$ .

The transition is manufactured in an aluminium block using standard milling machine techniques. Corners of the steps are rounded because of the milling tool diameter of 2.5 mm. Considering a higher electric field density in the centre part of the waveguide, the rounded corners have a negligible effect on the transmission coefficient of the transition. Due to higher demands on fabrication accuracy of millimetre-wave components, the dielectric layers of the proposed antenna are fabricated using a laser milling process. Subsequently, these antenna layers are fixed together by a 0.05-mm-thin adhesive tape that ensures stable fixation of the layers without unwanted air gaps. The input SIW is aligned to the transition using two screws driven into the aluminium block.



a



b

**Fig. 11** Radiation pattern of fabricated AC-MPAA fed by SIW at 60 GHz

a E-plane  
b H-plane

The reflection coefficient of the fabricated prototype measured at the input of the RWG WR15 is compared with the simulation results in Fig. 10. A good agreement between simulation and measurement is achieved while the fabricated antenna operates with the reflection coefficient lower than  $-10$  dB within the band from 59.4 to 60.5 GHz. It corresponds to the impedance bandwidth of 1.8% at the centre frequency of 60 GHz. The simulated impedance bandwidth of the antenna array is 2.5%.

The radiation pattern of the antenna array was measured in a shielded anechoic chamber. Due to the antenna holder, the radiation pattern was measured for angle theta from  $-90^\circ$  to  $90^\circ$ . During the measurement, the metal block of the transition was covered using a high-frequency absorbing material to suppress reflected waves. The measured E-plane ( $xz$ ) and H-plane ( $yz$ ) normalised radiation patterns are compared with the simulated ones in Fig. 11. Despite of the reflections from the transition were suppressed, a higher co-pol and x-pol components are obvious in H-plane radiation pattern. In both planes, the SLLs are below  $-23$  dB and the 3 dB beamwidth angle is  $14.5^\circ$ . The gain of the antenna array was measured by the comparison method using a reference antenna. The simulated and measured gain at 60 GHz is 22.0 and 21.6 dBi, respectively. The main reasons of the 0.4 dB gain difference are measurement uncertainty and higher dielectric losses of the used substrates than were included in the simulation.

## 5 Conclusion

In this paper, the AC-MPA fed by SIW was proposed in a  $6 \times 8$  array arrangement. Compared with a previously work on a uniform-fed linear AC-MPAA proposed by other authors [15], we implemented a desired amplitude distribution and described the procedure for the planar antenna array design to make the antenna array to be easy for design. The simulation results have been verified by measuring the fabricated prototype. Experimental results showed satisfactory agreement with the simulation.

Compared with the other work on SIW slot antennas [9–11], the obtained results of the proposed antenna array show higher gain with lower number of antenna elements. The antenna area is smaller and its design procedure is similar to the SIW slot antenna design. The MPAA fed by SIW could be utilised in a wide range of applications where SIW slot antennas are usually used, for example, as a multibeam antenna based on Rotman lens, etc.

## 6 Acknowledgement

Research described in this paper was financed by the Czech Ministry of Education in the frame of the National Sustainability Program under grant LO1401. For research, infrastructure of the SIX Center was used.

## 7 References

1 Daniels, R.C., Heath, R.W.: '60 GHz wireless communications: emerging requirements and design recommendations', *IEEE Veh. Tech. Mag.*, 2007, 2, (3), pp. 41–50

2 Cassivi, Y., Perregrini, L., Arcioni, P., et al.: 'Dispersion characteristics of substrate integrated rectangular waveguide', *IEEE Microw. Wirel. Compon. Lett.*, 2002, 12, (9), pp. 333–335

3 Xu, F., Wu, K.: 'Guided-wave and leakage characteristics of substrate integrated waveguide', *IEEE Trans. Microw. Theor. Tech.*, 2005, 53, (1), pp. 66–73

4 Yan, L., Hong, W., Wu, K., et al.: 'Investigations on the propagation characteristics of the substrate integrated waveguide based on the method of lines', *IEE Proc. Microw. Antennas Propag.*, 2005, 152, (1), pp. 35–42

5 Deslandes, D., Wu, K.: 'Accurate modeling, wave mechanisms, and design considerations of a substrate integrated waveguide', *IEEE Trans. Microw. Theor. Tech.*, 2006, 54, (6), pp. 2516–2526

6 Che, W., Deng, K., Wang, D., et al.: 'Analytical equivalence between substrate-integrated waveguide and rectangular waveguide', *IET Microw. Antennas Propag.*, 2008, 2, (1), pp. 35–41

7 Salehi, M., Mehrshahi, E.: 'A closed-form formula for dispersion characteristics of fundamental SIW mode', *IEEE Microw. Wirel. Compon. Lett.*, 2011, 21, (1), pp. 4–6

8 Bozzi, M., Georgiadis, A., Wu, K.: 'Review of substrate-integrated waveguide circuits and antennas', *IET Microw. Antennas Propag.*, 2011, 5, (8), pp. 909–920

9 Xu, J.F., Hong, W., Chen, P., et al.: 'Design and implementation of low sidelobe substrate integrated waveguide longitudinal slot array antennas', *IET Microw. Antennas Propag.*, 2009, 3, (5), pp. 790–797

10 Chen, X.P., Wu, K., Han, L., et al.: 'Low-cost high gain planar antenna array for 60 GHz band applications', *IEEE Trans. Antennas Propag.*, 2010, 58, (6), pp. 2126–2129

11 Navarro, D.V., Carrera, L.F., Baquero, M.: 'A SIW slot array antenna in Ku band'. Proc. 4th European Conf. on Antennas and Propagation, 2010, pp. 1–4

12 Elliott, R.S.: 'Antenna theory and design' (John Wiley & Sons, Inc., Hoboken (NJ), 2003, Revised edn., Chapter VIII)

13 Hao, Z.C., Hong, W., Chen, A., et al.: 'SIW fed dielectric resonator antennas'. Proc. IEEE MTT-S Int. Microw. Symp., 2006, pp. 202–205

14 Abdel-Wahab, W.M., Busuioc, D., Safavi-Nauini, S.: 'Millimeter-wave high radiation efficiency planar waveguide series-fed dielectric resonator antenna (DRA) array: analysis, design, and measurements', *IEEE Trans Antennas Propag.*, 2011, 59, (8), pp. 2834–2843

15 Abdel-Wahab, W.M., Safavi-Naeini, S., Busuioc, D.: 'Low cost microstrip patch antenna array using planar waveguide technology for emerging millimeter-wave wireless communication'. Proc. 14th Int. Symp. on Antenna Technology and Applied Electromagnetics and the American Electromagnetics Conf., 2010

16 Mikulasek, T., Lacik, J.: 'Microstrip patch antenna fed by substrate integrated waveguide'. Proc. 13th Int. Conf. on Electromagnetics in Advanced Applications, 2011, pp. 1209–1212

17 Mikulasek, T., Lacik, J.: 'Two feeding methods based on substrate integrated waveguide for microstrip patch antennas', *IET Microw. Antennas Propag.*, 2015, 9, (5), pp. 423–430

18 Ghassemi, N., Wu, K., Claude, S., et al.: 'Low-cost and high-efficient W-band substrate integrated waveguide antenna array made of printed circuit board process', *IEEE Trans. Antennas Propag.*, 2012, 60, (3), pp. 1648–1653

19 Abdel-Wahab, W.M., Safavi-Naeini, S., Busuioc, D.: 'Low cost 60 GHz millimeter-wave microstrip patch antenna array using low-loss planar feeding scheme'. Proc. IEEE Int. Symp. on Antennas and Propagation, 2011, pp. 508–511

20 Mikulasek, T., Georgiadis, A., Collado, A., et al.: '2 × 2 microstrip patch antenna array fed by substrate integrated waveguide for radar applications', *IEEE Antennas Wirel. Propag. Lett.*, 2013, 12, pp. 1287–1290

21 Ghassemi, N., Wu, K.: 'High-efficient patch antenna array for E-band gigabyte point-to-point wireless services', *IEEE Antennas Wirel. Propag. Lett.*, 2012, 11, pp. 1261–1264

22 Li, Y., Luk, K.M.: 'Low-Cost High-Gain and broadband substrate-Integrated-Waveguide-Fed patch antenna array for 60 GHz band', *IEEE Trans. Antennas Propag.*, 2014, 62, (11), pp. 5531–5538

23 Li, Y., Luk, K.M.: '60 GHz substrate integrated waveguide fed cavity-backed aperture-coupled microstrip patch antenna arrays', *IEEE Trans. Antennas Propag.*, 2015, 63, (3), pp. 1075–1085

24 Cheng, Y.J., Hong, W., Wu, K.: '94 GHz substrate integrated monopulse antenna array', *IEEE Trans. Antennas Propag.*, 2012, 60, (1), pp. 121–129

25 Lin, S., Yang, S., Fathy, A.E., et al.: 'Development of a novel UWB Vivaldi antenna array using SIW technology', *Progr. Electromagn. Res.*, 2009, 90, pp. 369–384

26 Mikulasek, T., Puskely, J., Lacik, J.: 'Design of radome-covered substrate integrated waveguide slot antenna array'. Proc. 8th European Conf. on Antennas and Propagation, 2013, pp. 1437–1441

27 Mikulasek, T., Lacik, J., Raida, Z.: 'SIW slot antennas utilized for 60 GHz channel characterization', *Microw. Opt. Tech. Lett.*, 2015, 57, (6), pp. 1365–1370

Copyright of IET Microwaves, Antennas & Propagation is the property of Institution of Engineering & Technology and its content may not be copied or emailed to multiple sites or posted to a listserv without the copyright holder's express written permission. However, users may print, download, or email articles for individual use.